BIOCHEMISTRY
including biophysical chemistry & molecular biology

Article

pubs.acs.org/biochemistry

The Dimerization Domain in Outer Segment Guanylate Cyclase Is a Ca^{2+}-Sensitive Control Switch Module

Patrick Zägel,[†] Daniele Dell'Orco,[§] and Karl-Wilhelm Koch*[,†,‡]

[†]Biochemistry Group, Department of Neurosciences, Carl von Ossietzky University Oldenburg, D-26111 Oldenburg, Germany

[‡]Research Center Neurosensory Science, Carl von Ossietzky University Oldenburg, D-26111 Oldenburg, Germany

[§]Department of Life Sciences and Reproduction, Section of Biological Chemistry, and Center for BioMedical Computing, University of Verona, Verona, Italy

Supporting Information

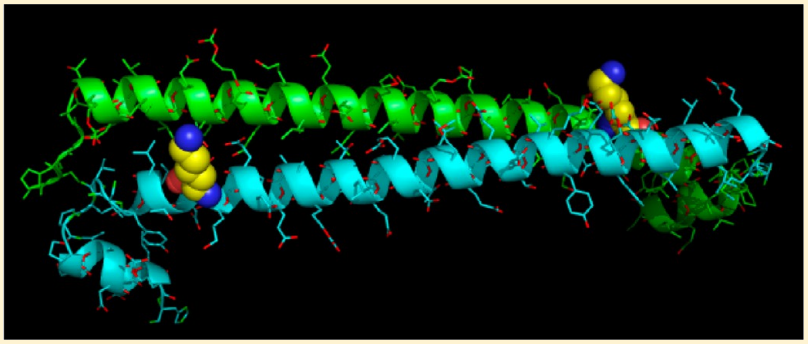

ABSTRACT: Membrane-bound guanylate cyclases harbor a region called the dimerization or linker domain, which aids the enzymes in adopting an optimal monomer−monomer arrangement for catalysis. One subgroup of these guanylate cyclases is expressed in rod and cone cells of vertebrate retina, and mutations in the dimerization domain of rod outer segment guanylate cyclase 1 (ROS-GC1, encoded by the *GUCY2D* gene) correlate with retinal cone-rod dystrophies. We investigate how a Q847L/K848Q double mutation, which was found in patients suffering from cone-rod dystrophy, and the Q847L and K848Q single-point mutations affect the regulatory mechanism of ROS-GC1. Both the wild type and mutants of heterologously expressed ROS-GC1 were present in membranes. However, the mutations affected the catalytic properties of ROS-GC1 in different manners. All mutants had higher basal guanylate cyclase activities but lower levels of activation by Ca^{2+}-sensing guanylate cyclase-activating proteins (GCAPs). Further, incubation with wild-type GCAP1 and GCAP2 revealed for all ROS-GC1 mutants a shift in Ca^{2+} sensitivity, but activation of the K848Q mutant by GCAPs was severely impaired. Apparent affinities for GCAP1 and GCAP2 were different for the double mutant and the wild type. Circular dichroism spectra of the dimerization domain showed that the wild type and mutants adopt a prevalently α-helical structure, but mutants exhibited lower thermal stability. Our results indicate that the dimerization domain serves as a Ca^{2+}-sensitive control module. Although it is per se not a Ca^{2+}-sensing unit, it seems to integrate and process information regarding Ca^{2+} sensing by sensor proteins and regulator effector affinity.

Regulation of vertebrate rod and cone phototransduction involves steps and feedback loops that critically depend on changes in intracellular Ca^{2+} levels.[1−3] Only two transport systems control the influx and efflux of Ca^{2+} in the outer segments of rod and cone cells, a cyclic nucleotide-gated channel (CNG) permeable to Na^+ and Ca^{2+} and a Na^+/K^+, Ca^{2+} exchanger.[4,5] The synchronous operation of the channel and exchanger maintains a Ca^{2+} concentration ranging from 250 nM in mice[6] to 800 nM in salamander[7] in the dark-adapted state. Illumination triggers the amplified hydrolysis of the second messenger cyclic GMP and the subsequent closure of CNG channels, which terminates Ca^{2+} influx, but not its extrusion via the operation of the exchanger leading to a decrease in the cytoplasmic Ca^{2+} concentration. These dynamic changes in intracellular Ca^{2+} concentration are sensed by Ca^{2+} sensor proteins, which regulate their targets in Ca^{2+}-dependent manners. One such group of Ca^{2+} sensors named guanylate cyclase-activating proteins (GCAPs) controls the activity of membrane-bound guanylate cyclases.[1−3]

Photoreceptors of different species express two, three, six, or up to eight different GCAP isoforms. The redundant expression of several GCAP forms in one cell type has initiated several *in vitro* and *in vivo* studies that aim to decipher possible differences in the Ca^{2+} sensing and regulatory properties.[8−13] Collectively, the results support a Ca^{2+}-relay model[14,15] in visual transduction that has the following key features: different GCAP isoforms (GCAP1 and GCAP2 in mammals, for example) exhibit different Ca^{2+} sensitivities and therefore regulate their target guanylate cyclase at different Ca^{2+} concentrations. When

Received: March 6, 2013
Revised: June 18, 2013
Published: July 2, 2013

dx.doi.org/10.1021/bi400288p | *Biochemistry* 2013, 52, 5065−5074

illumination of a photoreceptor cell leads to a decrease in the cytoplasmic Ca^{2+} concentration, first GCAP1 loses Ca^{2+} by exchange for Mg^{2+} because of its lower Ca^{2+} affinity and will start to activate the cyclase, while a further decrease in the Ca^{2+} concentration during the duration of a photoresponse triggers the activation of GCAP2.[10−14,16] This step-by-step activation process is linked to the adaptation properties of rod and cone cells, because different Ca^{2+} concentrations are adjusted under different light regimes.[17] This would allow the photoreceptor cell to synthesize cGMP in a very dynamic manner that is finely tuned to the currently required steady-state level of cGMP.

The importance of a fine-tuned sequential activation of photoreceptor guanylate cyclases by the GCAP Ca^{2+} sensors is also mirrored in mutations of the GCAP1 *GUCA1A* gene that cause cone dystrophies and cone-rod dystrophies (CORD). Most of the point mutations are located in or near the Ca^{2+}-binding sites EF-hand 3 and 4, and all these mutations cause severe dysfunction of the Ca^{2+} sensor properties of GCAP1, exhibiting in particular a shift to higher Ca^{2+} concentrations for the Ca^{2+}-dependent activation of guanylate cyclases.[18,19] Thus, impairment of correct Ca^{2+} sensing causes a significant distortion of the Ca^{2+}-relay activation mechanism.

In addition to mutations found in GCAP1, several mutations in the *GUCY2D* gene encoding the photoreceptor guanylate cyclase ROS-GC1 or GC-E correlate with retinal diseases like Leber's congenital amaurosis and cone-rod dystrophies.[20] It is necessary that two monomer ROS-GC1 molecules (Figure 1) dimerize to catalyze the synthesis of cGMP, and dimerization of ROS-GC1 is supposed to originate from the formation of a coiled-coil structure[21] within the dimerization domain (DD), which is distant from the cyclase catalytic domain (CCD) and harbors a "mutation hotspot" causing autosomal dominant cone dystrophy (CORD).[20] Previous biochemical analysis of some of these disease-causing point mutations has shown that the basal, i.e., nonstimulated, cyclase activity is significantly decreased,[22−24] but the mutants turned out to be more sensitive to activation by GCAP1 and GCAP2.[22,23] On the basis of the previously observed perturbations of the Ca^{2+}-relay model by GCAP1 mutants activating the wild-type (WT) form of the target cyclase, we ask in this investigation whether disease-related point mutations in ROS-GC1[25] also lead to an imbalance in cGMP−Ca^{2+} homeostasis. We studied the biochemical properties of ROS-GC1 mutants in cell culture systems reconstituted with purified GCAP forms and report here that mutations in the dimerization domain had consequences for Ca^{2+}-sensitive regulation by interacting Ca^{2+} sensors. We further show that, in spite of the high helical content, the ROS-GC1 dimerization domain per se might be folded in a manner that is significantly different from that of the expected coiled-coil motif, suggesting that rather than unfolding individual monomers, disease-associated mutants in that domain may destabilize supramolecular assemblies that are crucial for maintaining enzyme function.

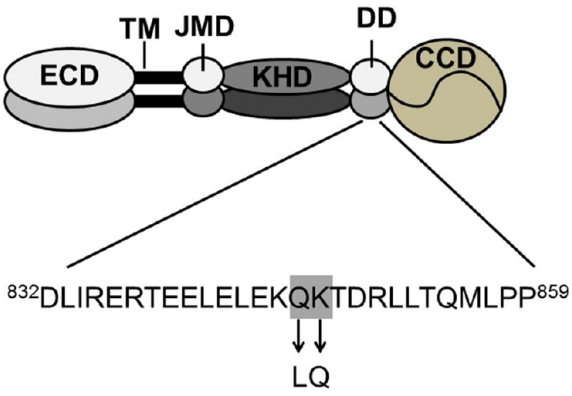

Figure 1. Structural topography of ROS-GC1. Amino acid sequence within the dimerization domain (DD) and localization of the point mutations that are investigated in this study. Other domains of ROS-GC1 are designated as the extracellular domain (ECD), corresponding to the intradiskal region when cyclases are expressed in rod outer segments, the transmembrane domain (TM), the juxtamembrane domain (JMD), the kinase homology domain (KHD), and the cyclase catalytic domain (CCD).

EXPERIMENTAL PROCEDURES

Cloning of Human ROS-GC1 Constructs. The cDNA of human ROS-GC1 was cloned into vector pIRES2-eGFP (Clontech), which is designed for parallel expression of the green fluorescent protein. For this purpose, the cDNA of human ROS-GC1 was amplified via polymerase chain reaction (PCR) using the forward primer 5′-AAAGCTAGCCACCATGACCG-CCTGCGCCCGCC-3′ and the reverse primer 5′-GCAGGAT-CCAGCATGTATGTGG-3′. The PCR product and vector were cut by NheI and BamHI, and the vector was dephosphorylated and ligated. The complete vector with the insert was used to transform XL1 blue *Escherichia coli* cells. DNA was prepared by using the DNA purification kit from Promega following the manufacturer's instructions.

Site-Directed Mutagenesis of Human ROS-GC1. Mutants of human ROS-GC1 were produced by using the following primers for PCR amplification: mutant Q847L, forward primer (5′-GCTGAAAAGCTGAAGACAGACCGG-3′) and reverse primer (5′-CCGGTCTGTCTTCAGCTTTTCCAGC-3′); mutant K848Q, forward primer (5′-GGAAAAGCAGCAGAC-AGACCGGCTG-3′) and reverse primer (5′-CAGCCGGTC-TGTCTGCTGCTTTTCC-3′); double mutant Q847L/K848Q, forward primer (5′-GCTGGAAAAGCTGCAGACA-GACCGGCTG-3′) and reverse primer (5′-CAGCCGGTCT-GTCTGCAGCTTTTCCAGC-3′). The PCR was performed on hROS-GC1 WT with the pIRES vector as a template. The PCR products were treated with T4 phosphatase for 1 h at 20 °C and then ligated with T4 ligase.

Cloning, Expression, and Purification of the Dimerization Domain. For biophysical studies of WT and mutant forms of the dimerization domain, we cloned the corresponding cDNA into the pET30a vector that is suitable for overexpression in bacteria. Therefore, forward (5′-AAACCATGGCTAACATCA-ACAAGGGCCGGAA-3′) and reverse (5′-AAAGAATTCACG-TCTTCAAGGCCTCAGCC-3′) primers were used in PCR amplification using WT or mutant hROS-GC1 in the pIRES vector as templates. For expression in *E. coli*, bacteria (BL21) were transformed by the corresponding DNA, and after a 5 mL preculture, cells were grown in 500 mL flasks (30 μg/mL kanamycin added) until an OD of 0.6 was reached. Expression was induced by adding 1 mM isopropyl β-D-thiogalactoside, and the cell suspension was incubated for 4 h at 37 °C while being agitated at 180 rpm. Cells were harvested by centrifugation at 5000×*g* for 10 min. The resulting pellet was stored at −80 °C until it was processed further. The pellet was suspended in 15 mL of 50 mM Tris (pH 7.4) containing DNase (final concentration of 5 units/mL) and lysozyme (100 μg/mL) by being shaken for 1 h at 30 °C. Insoluble material was removed by ultracentrifugation for 30 min at 30000 rpm and 4 °C (Sorvall, Thermo Fisher Scientific). The supernatant was

adjusted to final concentrations of 0.5 M NaCl, 1 mM DTT, 0.1 mM PMSF, and 20 mM imidazole and loaded on a 1 mL HisTrap column (GE Healthcare Life Sciences). Each of the dimerization domain constructs was eluted in a buffer consisting of 50 mM Tris (pH 7.4), 0.5 M NaCl, and 0.5 M imidazole. The tag of the fusion protein can be removed by treatment with enteropeptidase [enterokinase (Sigma-Aldrich Chemie GmbH, Munich, Germany)], but the product formed aggregates. Because we performed a few experiments with the tag-free protein, the procedure for obtaining it is briefly described. The eluate from the HisTrap column (see above) was diluted 10-fold with 50 mM Tris (pH 7.4), 0.5 M NaCl buffer, mixed with Ni-Sepharose (GE Healthcare Life Sciences) (4 mg of tagged protein per 100 μL of suspended sepharose) in a batch, and incubated overnight. The column material was sedimented and transferred into a column device. The column was washed extensively before the material (protein attached to column) was treated with enteropeptidase following the supplier's instructions (Sigma-Aldrich) for 18 h. Because the eluted protein sample was contaminated with the protease, the sample was further purified on a benzamidine column (Amersham Biosiences, Freiburg, Germany). Fractions containing the dimerization domain were pooled, and the buffer was changed to 50 mM NH_4HCO_3 when the samples were passed over a PD10 column (GE Healthcare Life Sciences). Samples were lyophilized for longer storage. The protein concentration was measured by recording the absorbance spectrum from 190 to 210 nm and taking the maximum for c (milligrams per milliliter) = $A_{max}/31$.

Heterologous Expression in HEK Cells. HEK flip 293 cells were cultivated in minimal essential medium under standard conditions as described previously[26] and harvested in 5 mM KCl, 20 mM $MgCl_2$, and 150 mM phosphate buffer (pH 7.2) (3−5 × 10^6 cells in 100 μL). For transfection, 5 μg of DNA was added and cells were electroporated with the CLB system (Lonza). Cells were flushed out of the electroporation cuvette by adding 1.5 mL of culture medium. The content of six cuvettes was poured onto one 9 cm plate and incubated for 24 h. The medium was changed and butyrate added (final concentration of 5 mM). After being incubated for 24 h, cells were harvested and sedimented by centrifugation at 1000×g for 5 min. The supernatant was discarded, and the pellet was frozen in liquid N_2 and stored at −80 °C. Cell membranes for further use in GC assays were thawed and resuspended in 0.5 mL of 10 mM Hepes-KOH (pH 7.4), 1 mM DTT, and a protease inhibitor cocktail (Sigma-Aldrich). After 30 min on ice, cells were sonicated (5 s, Branson sonifier B12, 80−100 W). The suspension was centrifuged for 10 min at 13000×, and the pellet was resuspended in 50 mM Hepes-KOH (pH 7.4), 50 mM KCl, 20 mM NaCl, and 1 mM DTT and stored at −80 °C.

Western Blotting. Sodium dodecyl sulfate−polyacrylamide gel electrophoresis (SDS−PAGE) and Western blotting were performed according to established procedures in the laboratory.[11] Primary antibody GC1#3[27] against ROS-GC1 was incubated with the membrane at a dilution of 1:2000 overnight. The secondary antibody was a goat anti-rabbit antibody coupled with horseradish peroxidase (Dianova Germany, provided at a concentration of 50% in glycerol) and was used at a dilution of 1:4000 after preincubation in a Tris-buffered saline/0.05% Tween 20/1% milk powder mixture.

Immunohistochemistry. Cells were grown on a poly-L-lysine-coated glass support by incubation for 24−48 h at 37 °C in minimal essential medium (see above). Afterward, cells were washed three times (5 min) in PBS (pH 7.4), fixed in 4% paraformaldehyde (pfa) and PBS (pH 7.4) for 10 min, and then again washed three times (5 min) with PBS (pH 7.4). For pfa/methanol fixation, pfa-fixed and -washed cells were incubated with methanol for 10 min at −20 °C and washed three times (5 min) with PBS (pH 7.4). Then, cells were incubated with 5% normal goat serum in PBS (pH 7.4) and 0.1% Triton X-100 for 1 h and subsequently incubated with the primary antibodies. As primary antibodies, we used anti-ROS-GC1 [1:100, ROS-GC1 (H-225), sc50512, rabbit polyclonal IgG (Santa Cruz Biotechnology)], anti-Na^+/K^+-ATPase [1:200, Na^+/K^+-ATPase, a (H-3), sc-48345, mouse monoclonal IgG_{2b} (Santa Cruz Biotechnology)], and anti-calnexin [1:200, calnexin (E-10), sc-46669, mouse monoclonal IgG_{2a} (Santa Cruz Biotechnology)]. Incubation was conducted for 24 h at room temperature in PBS (pH 7.4) and 0.1% Triton X-100. After being washed in PBS (pH 7.4), cells were incubated with secondary antibodies [1:200, donkey anti-rabbit antibody conjugated to Fura350 (Invitrogen); and 1:500, goat anti-mouse antibody conjugated with Dylight594 (Thermo Scientific)] for 3 h at room temperature in PBS (pH 7.4) and 0.1% Triton X-100. Finally, cells were washed again with PBS (pH 7.4) (3 × 5 min), sealed with Vectashield (Vector Laborates Inc., Burlingame, CA), and stored at 4 °C. Staining was visualized with a fluorescence microscope (EVOS Fl Fluoreszenz, Peqlab GmbH, Erlangen, Germany) using the Dapi- and/or RFP-LED-Light Cube.

Guanylate Cyclase Assay. Recombinant human ROS-GC1 in HEK cell membranes was measured as described previously for the bovine ortholog.[26] The effect of GCAPs on the activation profile was tested by adding purified bovine GCAP1 or GCAP2 at a saturating concentration of 10 μM to washed HEK cell membranes. In a second set of guanylate cyclase assays, we incubated recombinant ROS-GC1 in HEK cell membranes with increasing concentrations of GCAP1 and GCAP2 (0−20 μM) under conditions in which GCAPs were liganded with either Mg^{2+} (Ca^{2+}-free) or Ca^{2+} (incubation time of 30 min). The buffer composition was exactly as described previously[26] using final concentrations of 2 mM K_2H_2EGTA and 3.5 mM $MgCl_2$ for Mg^{2+}-liganded GCAPs and 33 μM free Ca^{2+} for Ca^{2+}-bound GCAPs. Evaluation of the data then yielded apparent affinities (EC_{50} values) of GCAPs for WT and mutant ROS-GC1. GCAPs were purified exactly as described previously.[26] The free Ca^{2+} concentration was varied from 1 nM to 33 μM by a Ca^{2+}-EGTA buffer system as described previously.[26] The free Ca^{2+} concentration in the micromolar (>33 μM) to millimolar range was adjusted by adding the required amount of $CaCl_2$. Stock solutions of Ca^{2+}-EGTA buffer were routinely checked for the free Ca^{2+} concentration by the fluorescent dye Fura-2.

Cross-Linking. HEK293 cell membranes containing WT and mutant ROS-GC1 were incubated with a final concentration of the bifunctional water insoluble cross-linker disuccinimidyl suberate (DSS) (Thermo Fisher Scientific, Rochester, IL) of 0.01 mM in a total volume of 10 μL (1 μL of membranes, 1 μL of 0.1 M DSS, and 8 μL of H_2O). The reaction was stopped after 10 min by adding 4 μL of 1 M Tris-HCl (pH 7.5). Samples, including the total reaction mixture, were added to SDS−PAGE sample buffer, heated to 95 °C for 5 min, and centrifuged at 13000× for 5 min before being analyzed by SDS−PAGE and Western blotting.

CD Spectroscopy. Far-UV CD spectra were recorded in the range of 200−250 nm using a Jasco V-710 CD spectrometer with a Peltier-type thermostated cell holder. Lyophilized samples of each peptide (WT and mutants) were resuspended

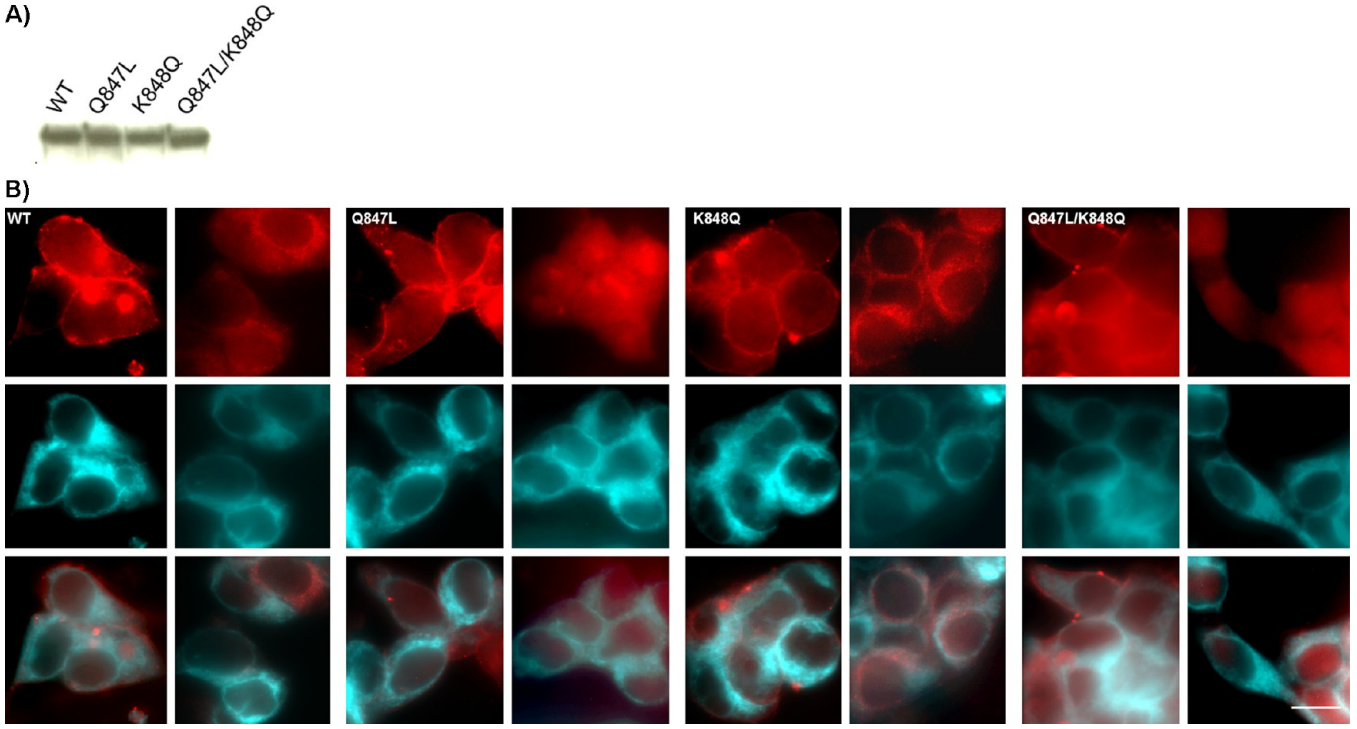

Figure 2. Expression and cellular localization of ROS-GC1 in HEK293 cells. (A) Western blot of HEK293 cells expressing human ROS-GC1, WT and mutants as indicated. Blots were probed with a primary antibody against ROS-GC1 (GC#3, 1:2000 dilution) and a secondary anti-rabbit antibody (1:4000) as described in Experimental Procedures. (B) For immunostaining, we used cells that were stably transfected with human ROS-GC1 constructs. Cells were probed with different antibodies: (top left panel of each ROS-GC1 construct) anti-Na^+/K^+-ATPase as the plasma membrane marker, with red staining, (top right panel) anti-calnexin antibodies as markers for the endoplasmic reticulum, (middle panels) anti-ROS-GC1 antibody, and (bottom panels) overlay of ROS-GC1 staining and membrane specific localization. Secondary antibodies are described in Experimental Procedures as well as visualization in a fluorescence microscope. Cells were fixed with either pfa (localization of plasma membrane) or pfa and methanol (endoplasmic reticulum). The scale bar is 10 μm.

in 5 mM Tris-HCl (pH 7.5) and 150 mM KCl to a final concentration of 0.5 mg/mL, and the spectra were recorded at 25 °C in a 1 mm quartz cuvette at a scan rate of 50 nm/min, a digital integration time of 4 s, and a bandwidth of 1 nm. Five spectra were accumulated for each sample and the results averaged.

Thermal denaturation of peptides was followed between 3 and 80 °C by recording the ellipticity at 222 nm (Θ_{222}) with a scan rate of 90 °C/h and a response time of 4 s. Thermal denaturation scans were fit to a theoretical two-state curve as previously illustrated[28] to assess the melting temperature (T_m). For each variant, a 250−200 nm CD spectrum was recorded 5−10 min after the maximal unfolding temperature (80 °C) had been reached, after which the sample was cooled to 25 °C and another spectrum was recorded (after 5 min) and compared with the initial one.

RESULTS

Expression of WT and Mutant ROS-GC1. A missense mutation in exon 13 of the *GUCY2D* gene leads to amino acid substitutions Q847L and K848Q in the translated gene product,[25] human ROS-GC1 (Figure 1). We investigated the biochemical consequences of this double mutation and each of the two amino acid substitutions separately (Q847L and K848Q). We created the corresponding mutants by site-directed mutagenesis and studied their properties after heterologous expression in HEK293 cells. Expressed proteins were located in the membrane fraction of HEK293 cells as seen by immunoblotting and probing of HEK293 membranes with an anti-ROS-GC1 antibody (Figure 2A). Cellular localization of ROS-GC1 WT and mutants was visualized by immunofluorescence. We localized the plasma membrane with an anti-Na^+/K^+-ATPase antibody (Figure 2B, top left panels for WT and each mutant, staining in red) and the endoplasmic reticulum with an anti-calnexin antibody (Figure 2B, always top right panels, staining in red). WT ROS-GC1 and its mutants were immunostained with the anti-ROS-GC1 antibody seen as the blue staining in the middle panels of Figure 2B. Please note absent or only weak background staining of the nucleus that is surrounded by membrane structures. An overlay with the cell membrane specific markers revealed that ROS-GC1 mainly colocalized with the endoplasmic reticulum (Figure 2B, bottom panels), which is in agreement with a previous observation by Peshenko et al.[29] of ROS-GC1 expression and colocalization in HEK293 cells.

Basic Activity Features. Cell membranes were further used to determine basic features of ROS-GC1 activity. These properties were the basal activities in the absence of GCAPs or activities at low (<10 nM) and high (33 μM) Ca^{2+} concentrations in the presence of either GCAP1 or GCAP2 (Figure 3A). The wild type and all mutants exhibited guanylate cyclase activity under all tested conditions. Thus, the mutations did not cause a loss of basal activity; instead all mutants, especially Q847L and double mutant Q847L/K848Q, showed an even higher basal activity than the WT. Differences in ROS-GC1 expression levels in HEK cells cannot be ascribed to these differences in cyclase activities, because we adjusted the amount of ROS-GC1 in all assay mixtures to nearly equal amounts by parallel immunoblotting (Figure 2A). Reconstitution with

dx.doi.org/10.1021/bi400288p | *Biochemistry* 2013, 52, 5065−5074

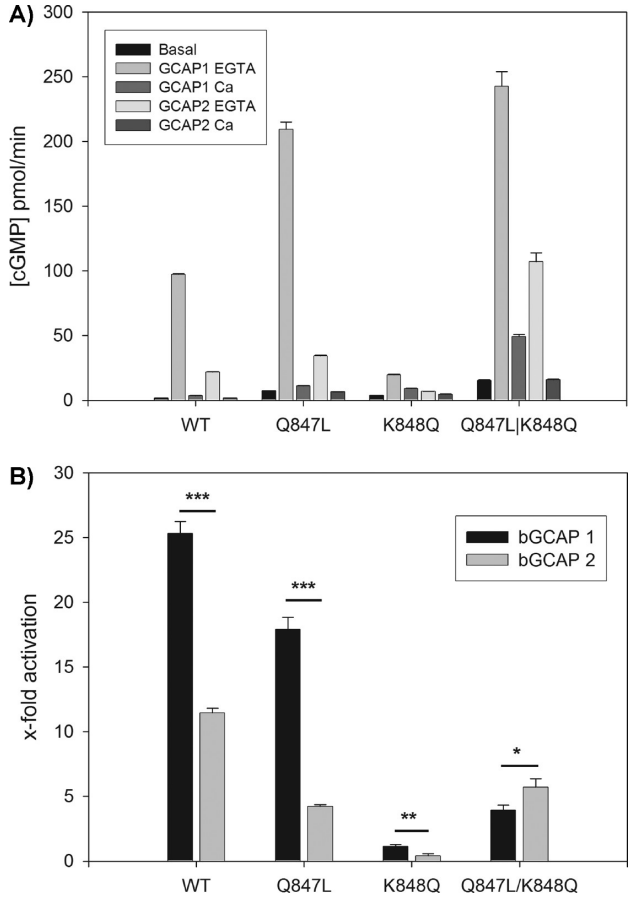

Figure 3. Guanylate cyclase activities of WT and ROS-GC1 mutants. (A) Membranes from HEK293 cells expressing human ROS-GC1 were reconstituted with Ca^{2+}-bound and Ca^{2+}-free (EGTA) GCAP1 or GCAP2 as indicated. GCAPs were present at a concentration of 10 μM, and the Ca^{2+} concentration was either 33 μM or <10 nM (EGTA). The amount of membranes for incubation was adjusted by Western blotting to yield equal amounts of WT and mutant guanylate cyclase (see Figure 2). Some error bars are too small to be visible because of the scale of the figure. (B) *x*-fold activation of ROS-GC1 forms by GCAP1 and GCAP2 is shown in a comparative diagram. The parameter "*x*-fold activation" is calculated from $(GC_{max} - GC_{min})/GC_{min}$, where GC_{max} is the maximal GC activity and GC_{min} is the minimal GC activity. Data are means ± the standard deviation of three different incubations (***$P < 0.001$; **$P < 0.01$; *$P < 0.05$).

GCAP1 or GCAP2 led to even larger changes in the activation pattern. In comparison to WT ROS-GC1, the Q847L mutant became more active in the presence of GCAP1, but GCAP2 activated WT and Q847L to almost the same extent (Figure 3A). A completely different picture emerged with the K848Q mutant that exhibited a much lower activity in the presence of Ca^{2+}-free GCAPs (Figure 3A). In contrast, the double mutant was highly active under all tested conditions, exceeding the values observed in the reconstitution experiments with the other mutants. Notably, Ca^{2+}-loaded GCAP2 did not fully deactivate the cyclases, which became particularly visible for the mutants.

A different way to analyze the activating properties of GCAPs is to compare the *x*-fold activation by calculating $(GC_{max} - GC_{min})/GC_{min}$.[11] While the values for WT ROS-GC1 reproduced well previous findings for *x*-fold activation between 10- and 25-fold (for a summary of previous work, see refs 1−3), all mutants showed a lower *x*-fold activation, revealing values in decreasing order: WT > Q847L > double mutant > K848Q (Figure 3B). This result was due to the significantly increased activity of the mutants in the presence of Ca^{2+}-loaded GCAPs and indicated that the Ca^{2+}-sensitive regulation of ROS-GC1 might be disturbed. Therefore, we investigated in more detail the Ca^{2+}-sensitive activation profiles of the ROS-GC1 mutants.

Ca^{2+}-Sensitive Activation Profile. Guanylate cyclases in rod and cone cells respond dynamically to changes in cytoplasmic Ca^{2+} concentration mediated by GCAPs. While the results in Figure 3 showed that the activity of all mutants was controlled by GCAPs, although leading to largely different activity amplitudes, the experiments could not clarify whether the Ca^{2+}-sensitive activation profiles differed from the one observed for the WT. Therefore, we measured the Ca^{2+}-sensitive activation profiles by reconstituting each mutant with either GCAP1 or GCAP2 at different free Ca^{2+} concentrations in the range from 10^{-9} to 10^{-3} M. Representative examples are shown in panels A and B of Figure 4. Half-maximal activation of each ROS-GC1/GCAP pair is assessed from plots as displayed in Figure 4 and is expressed as the IC_{50} (Table 1). Activation of wild-type ROS-GC1 by GCAP1 occurred at a higher free Ca^{2+} concentration (IC_{50} = 0.532 μM) than activation by GCAP2 (IC_{50} = 0.073 μM), which is similar to previous published work[10−13,16] and demonstrates the validity of our assay system. A noticeable difference was seen when the Q847L mutant was activated by GCAP2; the IC_{50} was shifted to much lower free Ca^{2+} concentrations, whereas the IC_{50} obtained with GCAP1 differed only modestly from the WT control. Rather surprising were, however, the activation profiles observed with the K848Q mutant. GCAP1 and GCAP2 operated in a reverse order: GCAP1 became more sensitive to Ca^{2+}, showing an IC_{50} of 0.187 μM, but GCAP2 turned into a regulator that was several orders of magnitude less sensitive to Ca^{2+} and remained a strong activator at 1 mM Ca^{2+} (filled triangles in Figure 4B). For determination of half-maximal activation, we took the cyclase activity at 1 mM Ca^{2+} as a minimum yielding an IC_{50} of 36.5 μM. We did not increase the free Ca^{2+} concentration beyond 1 mM, because higher Ca^{2+} concentrations would have interfered with the millimolar Mg^{2+}-GTP substrate concentrations. This strong disturbance of the GCAP-mediated Ca^{2+} sensitivity was partially compensated in the double mutant that was activated by GCAP1 at an approximately 5-fold higher Ca^{2+} concentration than by GCAP2 (Figure 4 and Table 1).

For simulating the cellular ROS-GC1 expression in patients suffering from retinal dystrophy, we mixed HEK cell membranes expressing WT with membranes harboring the double mutant. Equal amounts of ROS-GC1 forms were confirmed by parallel Western blotting. Subsequently, GCAP-mediated guanylate cyclase activities were measured. The IC_{50} in the presence of GCAP1 was shifted 2-fold to higher free Ca^{2+} concentrations with respect to the WT activation profile [IC_{50} = 1.2 μM (Figure S1A of the Supporting Information)]. A 2−3-fold shift was also observed with GCAP2 (Figure S1B of the Supporting Information).

Next we investigated whether the apparent relative affinities (EC_{50} values) of GCAPs for WT and the double mutant changed, when GCAPs are either Ca^{2+}-free (Mg^{2+}-liganded) or Ca^{2+}-loaded. As shown in Figure 4C, Mg^{2+}-loaded GCAP1 exhibited a higher affinity for the double mutant than for the WT (EC_{50} values of 0.6 μM for the mutant and 2.74 μM for the WT). Ca^{2+}-bound GCAP1 has instead very similar affinities for both WT and mutant ROS-GC1 (Figure 4D). The affinity of the double mutant for Mg^{2+}-loaded GCAP2 was ~10-fold lower than the affinity of GCAP1 for the mutant [EC_{50} = 7.6 μM

dx.doi.org/10.1021/bi400288p | *Biochemistry* 2013, 52, 5065−5074

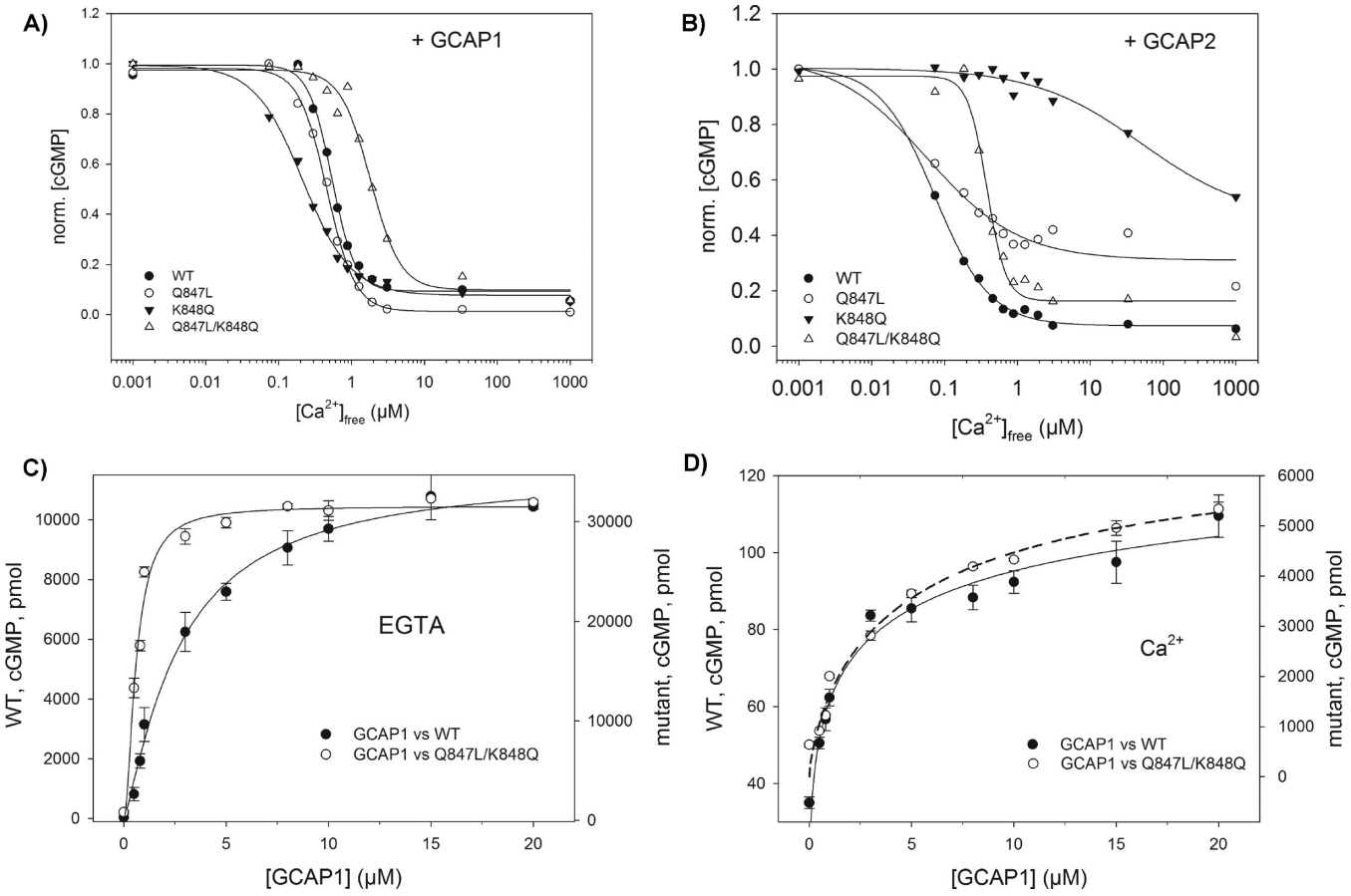

Figure 4. Ca^{2+}-dependent regulation of ROS-GC1 mutants by GCAP1 and GCAP2. Guanylate cyclase activities of different ROS-GC1 forms (see insets) were measured as a function of free Ca^{2+} concentration at a constant concentration of 10 μM GCAP1 (A) or GCAP2 (B). Activities are normalized to allow comparison of IC_{50} values ($[Ca^{2+}]_{free}$ at which activity is half-maximal). Data are representative of three sets of incubations. A summary of IC_{50} values is given in Table 1. (C) Determination of apparent affinities (EC_{50}) of WT (●) and double mutant Q847L/K848Q (○) for Ca^{2+}-free (Mg^{2+}-bound) GCAP1 and Ca^{2+}-bound GCAP1, where the free Ca^{2+} concentration was 33 μM (D). The amount of cGMP produced by ROS-GC1 in HEK cell membranes during a 30 min incubation is shown as a function of GCAP1 concentration.

Table 1. IC_{50} Values of Human WT ROS-GC1 and Its Mutants That Were Incubated with Myristoylated GCAP1 or GCAP2

	IC_{50} (μM)	
ROS-GC1	with GCAP1	with GCAP2
WT	0.532 ± 0.003	0.073 ± 0.0043
Q847L	0.469 ± 0.009	0.091 ± 0.015
K848Q	0.186 ± 0.011	36.485 ± 8.109
Q847L/K848Q	1.754 ± 0.039	0.369 ± 0.013

(Figure S2A of the Supporting Information)], but it was still 5-fold higher than for the WT. Ca^{2+}-loaded GCAP2 has a stronger inhibitory effect on WT ROS-GC1 than GCAP1, which is in agreement with previous observations[10] and thus resulted in very low activities close to the detection limit of our assay system (5−10 pmol) and a broad scattering of data. In contrast, the double mutant was activated by increasing Ca^{2+}-loaded GCAP2 concentrations with an EC_{50} of 5.5 μM (Figure S2B of the Supporting Information). In summary, affinities of GCAPs differ between the WT and mutants.

The mutations had no apparent effect on the dimerization of ROS-GC1, which we tested by using the bifunctional cross-linker DSS and subsequent analysis by SDS−PAGE and Western blotting (Figure 5). The staining pattern of ROS-GC1 was nearly identical for the WT and all mutants, and the blot showed the monomer at ~110 kDa, a dimer at ~220 kDa, and higher-molecular mass products representing cross-linked oligomers. In the absence of the cross-linker (Figure 5, right panel), we detected only the monomer after SDS−PAGE and also some high-molecular mass oligomers, but at a much lower intensity.

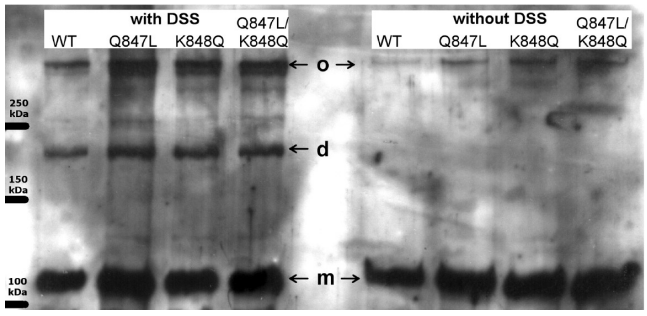

Figure 5. Cross-linking of WT and mutant ROS-GC1. HEK293 cell membranes containing heterologously expressed ROS-GC1 forms were incubated with the cross-linker DSS. After the reaction had been stopped, samples were analyzed by SDS−PAGE as indicated for each lane and proteins were subsequently probed by Western blotting using the anti-GC1#3 antibody (1:2000 dilution). Monomer (m), dimer (d), and oligomer (o) bands are indicated.

dx.doi.org/10.1021/bi400288p | *Biochemistry* 2013, 52, 5065−5074

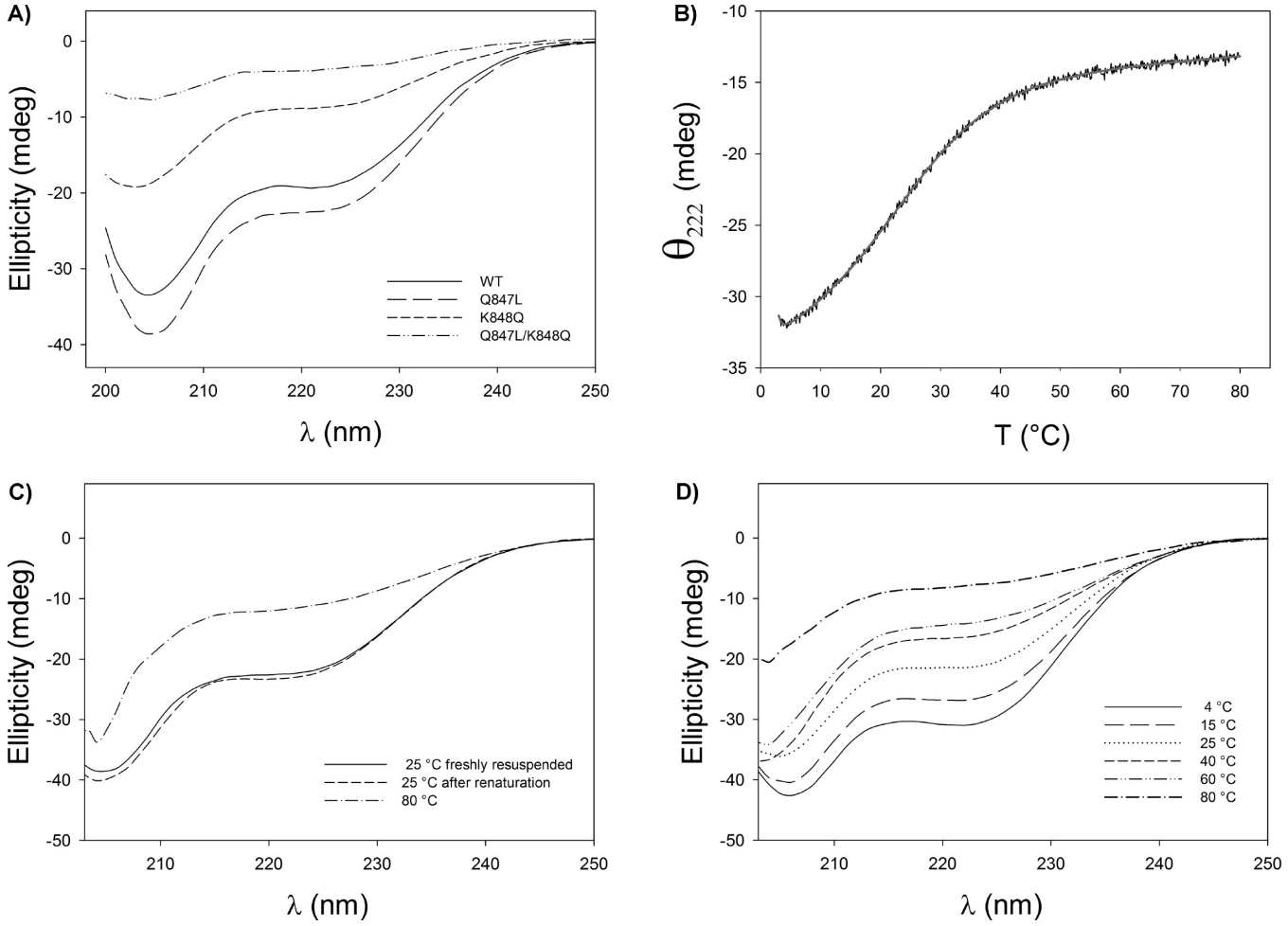

Figure 6. CD spectroscopic results for ROS-GC1 dimerization domain peptides. (A) Far-UV CD spectra recorded at 25 °C of 0.5 mg/mL WT and Q847L, K84Q, and Q847L/K848Q peptides from the ROS-GC1 dimerization domain. (B) Example of a thermal unfolding curve (WT peptide) obtained by recording the CD signal at 222 nm in the range of 3−80 °C. The dark gray curve refers to the computer-fitted curve that yields T_m. (C) Examples of CD spectra after thermal unfolding (80 °C) and after cooling the unfolded peptide to 25 °C, and comparison with that of the freshly resuspended peptide before unfolding at 25 °C. Data refer to the Q847L mutant. (D) CD spectra obtained for the WT peptide (0.5 mg/mL) at different temperaures in the range of 4−80 °C. The $\Theta_{222}/\Theta_{208}$ ratios were 0.76 (4 °C), 0.71 (15 °C), 0.65 (25 °C), 0.57 (40 °C), and 0.53 (60 and 80 °C).

An identical pattern was previously observed for bovine ROS-GC1.[23]

Folding of the Dimerization Domain. Correct folding of the GC dimerization domain is necessary for proper guanylate cyclase activities. We therefore looked for possible differences in the folding and assembly of the dimerization domain in WT and mutant ROS-GC1. Expression and purification of the isolated dimerization domains relating to amino acids N807−T867 resulted in peptides with a strong tendency to form aggregates. To prevent aggregation, we expressed and purified these peptides as tagged fusion proteins, which could be employed in a CD spectroscopic analysis.

The WT and mutants clearly had a helical content, but CD spectra were not typical for an α-helical protein (Figure 6A), because the $\Theta_{222}/\Theta_{208}$ ratio for the WT and the mutants was equal to 0.66, hence far from the typical values of both all-α structures (∼0.85) and coiled-coil motifs (∼1.02).[30,31] Despite the comparable concentration, resuspended peptides showed CD spectra with very similar shapes but significantly different intensities (Figure 6A), probably due to a substantially different proportion of peptides folded and correctly assembled in each case. Thus, the results clearly show that the point mutations do not disrupt the individual folding of the peptides but may affect the propensity for forming supramolecular assemblies.

To investigate the effects of the mutations on peptide stability, thermal unfolding of all variants was monitored by recording the change in ellipticity Θ at 222 nm as a function of temperature in the range of 3−80 °C (Figure 6B). Clear differences in thermal stability were observed between the WT and K848Q and double-mutant proteins, but a much smaller difference was measured between the WT and Q847L. Melting temperature T_m (in brackets) decreased in the following order: WT (30.5 °C) > Q847L (28.6 °C) > K848Q (21.0 °C) > Q847L/K848Q (17.2 °C). However, the thermal unfolding process was for all tested proteins completely reversible, as reported for example in Figure 6C for the Q847L mutant. For the WT case, spectra were recorded in the range of 4−80 °C to monitor the residual ellipticity as measured by the $\Theta_{222}/\Theta_{208}$ ratio (Figure 6D). Interestingly and in spite of the full reversibility of the thermal unfolding process, such a ratio monotonically decreased from 0.76 (4 °C) to 0.53 (80 °C), indicative of a likely temperature-dependent association or oligomerization of the peptide.

dx.doi.org/10.1021/bi400288p | *Biochemistry* 2013, 52, 5065−5074

DISCUSSION

Retinal diseases like cone-rod dystrophies and Leber's congenital amaurosis correlate often with mutations in the *GUCY2D* gene encoding ROS-GC1 in photoreceptor cells.[20−25] The dimerization domain in ROS-GC1 appears to be particularly prone to mutations that affect the catalytic properties of the cyclase, because it harbors several of the known mutations described in patients suffering from retinal diseases. We started this work to gain insight into the regulatory mechanism of ROS-GC1 by investigating the biochemical properties of three mutations, one being present as a double mutation in two patients diagnosed with an autosomal dominant cone-rod dystrophy.[25] The mutations affected the catalytic properties of ROS-GC1 in different manners. (1) All mutants had a higher basal guanylate cyclase activity but lower *x*-fold activation. (2) Incubation with WT GCAP1 and GCAP2 revealed for all ROS-GC1 mutants a shift in Ca^{2+} sensitivity. (3) Activation of the K848Q mutant by GCAPs was severely impaired.

Any consequence of the mutations on the basal activity could have been predicted, because it is known from previous studies that the correct alignment of the guanylate cyclase dimer is necessary for an efficient catalysis.[21,23,32] Moreover, mutations close to the location of the mutations investigated here impaired the correct formation of the monomer−monomer interface and affected the catalytic activity.[23] In contrast, our cross-linking studies of our ROS-GC1 samples showed that dimer formation was not disturbed. The CD spectra of the dimerization domain further confirmed that the general folding was intact, although the mutants were less thermally stable than the WT. Similar to what was found by Saha et al.,[33] who recorded CD spectra of a 25-amino acid peptide of the GC-C dimerization domain sharing a high degree of sequence similarity with ROS-GC1, the secondary structure observed here does not reflect that of a typical coiled-coil motif, but a helical content is observed that dynamically changes upon mutation or a change in temperature. Overall, our spectroscopic data are in line with the hypothesis that the ROS-GC1 dimerization domain is capable of self-association and possibly oligomerization, a process that is clearly affected by point mutations and eventually results in mutants exhibiting a higher basal cyclase activity. Less predictable was, however, the fact that the Ca^{2+}-sensitive regulation of ROS-GC1 mutants by GCAP1 and GCAP2 was shifted. The K848Q mutant was even constitutively active in the presence of GCAP2 at high Ca^{2+} concentrations (Figure 4B), although the activity was remarkably decreased. The phenomena of shifted Ca^{2+} sensitivity and constitutive activation of photoreceptor guanylate cyclases had previously been observed with GCAP1 mutants correlating with cone-rod diseases. GCAP1 mutants were severely disturbed and showed differences in Ca^{2+} binding affinity, structural stability, and Ca^{2+}-induced conformational changes, when compared with WT GCAP1.[19,28,34,35] In such a case, the Ca^{2+} sensor is affected and as a consequence the regulation of the target enzyme, as well. In this work, the defect is located in the target and not in the sensor.

Photoreceptor cells of patients suffering from cone dystrophies caused by the Q847L/K848Q double mutation probably have a shifted Ca^{2+} sensitivity of the cyclase, in line with the shift observed in our study, when we assayed membranes with a 1:1 WT:Q847L/K848Q ratio (Supporting Information). A cellular consequence would be that ROS-GC1 turns into an active enzyme at intracellular Ca^{2+} concentrations that far exceed the dark value (see the introductory section), leading to an overall distortion of the cGMP-Ca^{2+} homeostasis. In addition, the mutation might decrease the dynamic response range of ROS-GC1, because the double mutant had significantly decreased *x*-fold activation (Figure 3B) despite an increase in activity when compared to that of the WT (Figure 3A).

A very critical amino acid position in the dimerization domain is R838 that is located N-terminally to Q847, and R → C, R → S, and R → H point mutations have been linked to autosomal dominant cone-rod dystrophies.[20−24,35,36] Biochemical analysis of these mutants also showed an altered Ca^{2+} sensitivity of GCAP1 regulation with a shift to higher Ca^{2+} concentrations.[35,36] A double and a triple mutation involving R838 (E837D/R838S and E837S/R838C/T839M)[21,23] had similar consequences; i.e., higher Ca^{2+} concentrations are needed for inactivation by GCAP1. Another study, in which point mutations were separately investigated, reported that E837 or the R838C mutant became more sensitive to either GCAP2 or GCAP1, respectively.[22] The triple mutation had a severe effect on the basal cyclase activity, which could not be compensated by the action of GCAP1 or GCAP2. This damage could be related to a massive disturbance in dimer formation.[23]

Peshenko et al.[37] investigated in a study of the R838S ROS-GC1 mutant whether the observed shift in Ca^{2+} sensitivity (see above) originates from different apparent affinities of WT and mutant ROS-GC1 for Ca^{2+}-free (Mg^{2+}-bound) and Ca^{2+}-loaded GCAP1. The authors confirm a model in which the relative affinities of the Ca^{2+} sensor (GCAP1) for the effector also influence the Ca^{2+}-sensitive regulation of the effector. Our results in panels C and D of Figure 4 are in agreement with their conclusion, because we also observed that the apparent affinity of Mg^{2+}-loaded GCAP1 (and GCAP2) was higher for the mutant than for the WT.

A previous site-directed mutagenesis study of receptor guanylate cyclase type C had defined a regulatory role for the dimerization or linker region, and Saha et al.[32] concluded in their study that this region operates to transduce the extracellular ligand-induced activation to the CCD. Membrane-bound guanylate cyclases share a high degree of homology in the dimerization/linker region, and in a comparative study of receptor guanylate cyclases, it was further suggested that this region functions as a switch to prevent constitutive activation of downstream signaling domains.[38] Further support for this hypothesis came from a recent study by Duda et al.[39] showing that deletion of the signaling domain in bovine ROS-GC1 abolished signaling by GCAP1, but not by GCAP2. It is worth noting that mutations in regions outside of the dimerization domain, which have been investigated so far, show no change in Ca^{2+} sensitivity (LCA1-related mutations S248W and R1091x[40]) or failed to become activated by GCAPs.[41,42] Mutations in the extracellular domain (C105Y and L325P) or in the CCD (P858S and L954P) cause moderately and markedly reduced basal and GCAP-stimulated activity.[43]

GCAP1 and GCAP2 regulate ROS-GC1 activity by binding to interaction sites that are either upstream or downstream of the dimerization domain.[39,41,42] Thus, the change in Ca^{2+} sensitivity cannot be explained by binding of the Ca^{2+} sensor with a different affinity for the mutated site thereby causing a change in the interaction process. However, the difference in apparent affinities of GCAPs for WT and mutant ROS-GC1 indicates that a mutation distant from the interaction site can well shift the affinity of the Ca^{2+}-sensitive regulator. Therefore, the dimerization domain operates as a regulatory module and appears like a Ca^{2+}-sensitive control switch, which needs a correct

arrangement of its monomer−monomer interface for precise information processing.[21,33] The disturbance of this monomer−monomer alignment can cause changes in relative affinities for Ca^{2+}-sensing regulators, which further leads to a shift in catalytic properties.

■ ASSOCIATED CONTENT

Supporting Information

Ca^{2+}-dependent regulation of WT and double-mutant ROS-GC1 present in a 1:1 ratio (Figure S1) and determination of apparent affinities (EC_{50}) of WT and double mutant Q847L/K848Q for Ca^{2+}-free (Mg^{2+}-bound) GCAP2 and Ca^{2+}-bound GCAP2 (Figure S2). This material is available free of charge via the Internet at http://pubs.acs.org.

■ AUTHOR INFORMATION

Corresponding Author

*Phone: +49-441-798-3640, E-mail: karl.w.koch@uni-oldenburg.de.

Funding

This study was supported by a grant from the Deutsche Forschungsgemeinschaft (DFG) to K.-W.K. (KO948/10-1).

Notes

The authors declare no competing financial interest.

■ ACKNOWLEDGMENTS

We thank Jutta Appelt for technical assistance in the cell culture laboratory and Dr. Alexander Scholten for fruitful discussions.

■ ABBREVIATIONS

CD, circular dichroism; CORD, cone-rod dystrophy; GCAP, guanylate cyclase-activating protein; PAGE, polyacrylamide gel electrophoresis; ROS-GC1, rod outer segment guanylate cyclase; WT, wild type.

■ REFERENCES

(1) Stephen, R., Filipek, S., Palczewski, K., and Sousa, M. C. (2008) Ca^{2+}-dependent regulation of phototransduction. *Photochem. Photobiol. 84*, 903−910.

(2) Koch, K.-W., Duda, T., and Sharma, R. K. (2010) Ca^{2+}-modulated vision-linked ROS-GC guanylate cyclase transduction machinery. *Mol. Cell. Biochem. 334*, 105−115.

(3) Dizhoor, A. M., Olshevskaya, E. V., and Peshenko, I. V. (2010) Mg^{2+}/Ca^{2+} cation binding cycle of guanylyl cyclase activating proteins (GCAPs): Role in regulation of photoreceptor guanylyl cyclase. *Mol. Cell. Biochem. 334*, 117−124.

(4) Kaupp, U. B., and Seifert, R. (2002) Cyclic nucleotide-gated ion channels. *Physiol. Rev. 82*, 769−824.

(5) Luo, D. G., Xue, T., and Yau, K.-W. (2008) How vision begins: An odyssey. *Proc. Natl. Acad. Sci. U.S.A. 105*, 9855−9862.

(6) Woodruff, M. L., Sampath, A. P., Matthews, H. R., Krasnoperova, N. V., Lem, J., and Fain, G. L. (2002) Measurement of cytoplasmic calcium concentration in the rods of wild-type and transducin knock-out mice. *J. Physiol. 542.3*, 843−854.

(7) Nakatani, K., Chen, C., Yau, K.-W., and Koutalos, Y. (2002) Calcium and phototransduction. *Adv. Exp. Med. Biol. 514*, 1−20.

(8) Mendez, A., Burns, M. E., Sokal, I., Dizhoor, A. M., Baehr, W., Palczewski, K., Baylor, D., and Chen, J. (2001) Role of guanylate cyclase-activating proteins (GCAPs) in setting the flash sensitivity of rod photoreceptors. *Proc. Natl. Acad. Sci. U.S.A. 98*, 9948−9953.

(9) Burns, M. E., Mendez, A., Chen, J., and Baylor, D. A. (2002) Dynamics of cyclic GMP synthesis in retinal rods. *Neuron 36*, 81−91.

(10) Hwang, J.-Y., Lange, C., Helten, A., Höppner-Heitmann, D., Duda, T., Sharma, R. K., and Koch, K.-W. (2003) Regulatory modes of rod outer segment membrane guanylate cyclase differ in catalytic efficiency and Ca^{2+}-sensitivity. *Eur. J. Biochem. 270*, 3814−3821.

(11) Scholten, A., and Koch, K.-W. (2011) Differential calcium signaling by cone specific guanylate cyclase-activating proteins from the zebrafish retina. *PLoS One 6*, e23117.

(12) Peshenko, I. V., Olshevskaya, E. V., Savchenko, A. B., Karan, S., Palczewski, K., Baehr, W., and Dizhoor, W. (2011) Enzymatic properties and regulation of the native isozymes of retinal membrane guanylyl cyclase (RetGC) from mouse photoreceptors. *Biochemistry 50*, 5590−5600.

(13) Makino, C. L., Wen, X. H., Olshevskaya, E. V., Peshenko, I. V., Savchenko, A. B., and Dizhoor, A. M. (2012) Enzymatic relay mechanism stimulates cyclic GMP synthesis in rod photoresponse: Biochemical and physiological study in guanylyl cyclase activating protein 1 knockout mice. *PLoS One 7*, e47637.

(14) Koch, K.-W., and Dell'Orco, D. (2013) A Calcium-Relay Mechanism in Vertebrate Phototransduction. *ACS Chem. Neurosci. 4*, 909−917.

(15) Burgoyne, R. D. (2007) Neuronal calcium sensor proteins: Generating diversity in neuronal Ca^{2+} signaling. *Nat. Rev. Neurosci. 8*, 182−193.

(16) Peshenko, I. V., and Dizhoor, A. M. (2004) Guanylyl cyclase-activating proteins (GCAPs) are Ca^{2+}/Mg^{2+} sensors: Implications for photoreceptor guanylyl cyclase (RetGC) regulation in mammalian photoreceptors. *J. Biol. Chem. 279*, 16903−16906.

(17) Pugh, E. N., Jr., and Lamb, T. D. (2000) Phototransduction in vertebrate rods and cones: Molecular mechanisms of amplification, recovery and light adaptation. In *Handbook of Biological Physics* (Stavenga, D. G., DeGrip, W. J., Pugh, E. N., Jr. , Eds.)Vol. *3*, pp 183−255, Elsevier Science BV, Amsterdam.

(18) Behnen, P., Dell'Orco, D., and Koch, K.-W. (2010) Involvement of the calcium sensor GCAP1 in hereditary cone dystrophies. *Biol. Chem. 391*, 631−637.

(19) Hunt, D. M., Buch, P., and Michaelides, M. (2010) Guanylate cyclases and associated activator proteins in retinal disease. *Mol. Cell. Biochem. 334*, 157−168.

(20) Kitiratschky, V. B., Wilke, R., Renner, A. B., Kellner, U., Vadalà, M., Birch, D. G., Wissinger, B., Zrenner, E., and Kohl, S. (2008) Mutation analysis identifies GUCY2D as the major gene responsible for autosomal dominant progressive cone degeneration. *Invest. Ophthalmol. Visual Sci. 49*, 5015−5023.

(21) Ramamurthy, V., Tucker, C., Wilkie, S. E., Daggett, V., Hunt, D. M., and Hurley, J. B. (2001) Interactions within the coiled-coil domain of RetGC-1 guanylyl cyclase are optimized for regulation rather than for high affinity. *J. Biol. Chem. 276*, 26218−26229.

(22) Duda, T., Krishnan, A., Venkataraman, V., Lange, C., Koch, K.-W., and Sharma, R. K. (1999) Mutations in the rod outer segment membrane guanylate cyclase (ROS-GC1) in a cone-rod dystrophy cause defects in calcium signaling. *Biochemistry 38*, 13912−13919.

(23) Duda, T., Venkataraman, V., Jankowska, A., Lange, C., Koch, K.-W., and Sharma, R. K. (2000) Impairment of the Rod Outer Segment Membrane Guanylate Cyclase Dimerization in a Cone-Rod Dystrophy Results in Defective Calcium Signaling. *Biochemistry 39*, 12522−12533.

(24) Wilkie, S. E., Newbold, R. J., Deery, E., Walker, C. E., Stinton, I., Ramamurthy, V., Hurley, J. B., Bhattacharya, S. S., Warren, M. J., and Hunt, D. M. (2000) Functional characterization of missense mutations at codon 838 in retinal guanylate cyclase correlates with disease severity in patients with autosomal dominant cone-rod dystrophy. *Hum. Mol. Genet. 9*, 3065−3073.

(25) Yoshida, S., Yamaji, Y., Yoshida, A., Kuwahara, R., Yamamoto, K., Kubata, T., and Ishibashi, T. (2006) Novel triple missense mutations of GUCY2D gene in Japanese family with cone-rod dystrophy: Possible use of genotyping microarray. *Mol. Vision 12*, 1558−1564.

(26) Koch, K.-W., and Helten, A. (2008) Guanylate cyclase-based signaling in photoreceptors and retina. In *Signal Transduction in the Retina* (Fliesler, S. J., and Kisselev, O. G., Eds.) Chapter 6, pp 121−143, CRC Press, Boca Raton, FL.

(27) Helten, A., Säftel, W., and Koch, K.-W. (2007) Expression level and activity profile of membrane bound guanylate cyclase type 2 in rod outer segments. *J. Neurochem. 103*, 1439−1446.

(28) Dell'Orco, D., Behnen, P., Linse, S., and Koch, K.-W. (2010) Calcium binding, structural stability and guanylate cyclase activation in GCAP1 variants associated with human cone dystrophy. *Cell. Mol. Life Sci. 67*, 973−984.
(29) Peshenko, I. V., Olshevskaya, E., and Dizhoor, A. M. (2008) Binding of guanylyl cyclase activating protein 1 (GCAP1) to retinal guanylyl cyclase (RetGC1). *J. Biol. Chem. 283*, 21747−21757.
(30) Choy, N., Raussens, V., and Narayanaswami, V. (2003) Inter-molecular coiled-coil formation in human apolipoprotein E C-terminal domain. *J. Mol. Biol. 334*, 527−539.
(31) Franke, J. D., Dong, F., Rickoll, W. L., Kelley, M. J., and Kiehart, D. P. (2005) Rod mutations associated with MYH9-related disorders disrupt nonmuscle myosin-IIA assembly. *Blood 105*, 161−169.
(32) Liu, Y., Ruoho, A. E., Rao, V. D., and Hurley, J. B. (1997) Catalytic mechanism of the adenylyl and guanylyl cyclases: Modeling and mutational analysis. *Proc. Natl. Acad. Sci. U.S.A. 94*, 13414−13419.
(33) Saha, S., Biswas, K. H., Kondapalli, C., Isloor, N., and Visweswariah, S. S. (2009) The linker region in receptor guanylyl cyclases is a key regulatory module: Mutational analysis of guanylyl cyclase C. *J. Biol. Chem. 284*, 27135−27145.
(34) Olshevskaya, E. V., Peshenko, I. V., Savchenko, A. B., and Dizhoor, A. M. (2012) Retinal guanylyl cyclase isozyme 1 is the preferential in vivo target for constitutively active GCAP1 mutants causing congenital degeneration of photoreceptors. *J. Neurosci. 32*, 7208−7217.
(35) Kitiratschky, V. B. D., Behnen, P., Kellner, U., Heckenlively, J. R., Zrenner, E., Jägle, H., Kohl, S., Wissinger, B., and Koch, K.-W. (2009) Mutations in the GUCA1A gene involved in hereditary cone dystrophies impair calcium-mediated regulation of guanlyate cyclase. *Hum. Mutat. 30*, E782−E796.
(36) Tucker, C. L., Woodcock, S. C., Kelsell, R. E., Ramamurthy, V., Hunt, D. M., and Hurley, J. B. (1999) Biochemical analysis of a dimerization domain mutation in RetGC-1 associated with dominant cone-rod dystrophy. *Proc. Natl. Acad. Sci. U.S.A. 96*, 9039−9044.
(37) Peshenko, I. V., Moiseyev, G. P., Olshevskaya, E. V., and Dizhoor, A. M. (2004) Factors that determine Ca^{2+} sensitivity of photoreceptor guanylyl cyclase. Kinetic analysis of the interaction between the Ca^{2+}-bound and the Ca^{2+}-free guanylyl cyclase activating proteins (GCAPs) and recombinant photoreceptor guanylyl cyclase 1 (RetGC-1). *Biochemistry 43*, 13796−13804.
(38) Anantharaman, V., Balaji, S., and Aravind, L. (2006) The signaling helix: A common functional theme in diverse signaling proteins. *Biol. Direct 1*, 25.
(39) Duda, T., Pertzev, A., and Sharma, R. K. (2012) Differential Ca^{2+} sensor guanylate cyclase activating protein modes of photo-receptor rod outer segment membrane guanylate cyclase signaling. *Biochemistry 51*, 4650−4657.
(40) Jacobson, S. G., Cideciyan, A. V., Peshenko, I. V., Sumaroka, A., Olshevskaya, E. V., Cao, L., Schwartz, S. B., Roman, A. J., Olivares, M. B., Sadigh, S., Yau, K. W., Heon, E., Stone, E. M., and Dizhoor, A. M. (2012) Determining consequences of retinal membrane guanylyl cyclase (RetGC1) deficiency in human Leber congenital amaurosis en route to therapy: Residual cone-photoreceptor vision correlates with biochemical properties of the mutants. *Hum. Mol. Genet. 22*, 168−183.
(41) Duda, T., Venkataraman, V., Goraczniak, R., Lange, C., Koch, K.-W., and Sharma, R. K. (1999) Functional Consequences of a Rod Outer Segment Membrane Guanylate Cyclase (ROS-GC1) Gene Mutation Linked with Lebeŕs Congenital Amaurosis. *Biochemistry 38*, 509−515.
(42) Peshenko, I. V., Olshevskaya, E. V., Yao, S., Ezzeldin, H. H., Pittler, S. J., and Dizhoor, A. M. (2010) Activation of retinal guanylyl cyclase RetGC1 by GCAP1: Stoichiometry of binding and effect of new LCA-related mutations. *Biochemistry 49*, 709−717.
(43) Tucker, C. L., Ramamurthy, V., Pina, A. L., Loyer, M., Dharmaraj, S., Li, Y., Maumenee, I. H., Hurley, J. B., and Koenekoop, R. K. (2004) Functional analyses of mutant recessive GUCY2D alleles identified in Leber congenital amaurosis patients: Protein domain comparisons and dominant negative effects. *Mol. Vision 10*, 297−303.